Biochemistry and Biophysics Reports 11 (2017) 1–8

Contents lists available at ScienceDirect

Biochemistry and Biophysics Reports

journal homepage: www.elsevier.com/locate/bbrep

Global mapping of post-translational modifications on histone H3 variants in mouse testes

Ho-Geun Kwak, Takehiro Suzuki, Naoshi Dohmae*

Biomolecular Characterization Unit, RIKEN Center for Sustainable Resource Science, 2-1 Hirosawa, Wako 351-0198, Japan

ARTICLE INFO

Keywords:
Testis-specific H3 histone
Post-translational modification
Mass spectrometry
Spermatogenesis

ABSTRACT

Mass spectrometry (MS)-based characterization is important in proteomic research for verification of structural features and functional understanding of gene expression. Post-translational modifications (PTMs) such as methylation and acetylation have been reported to be associated with chromatin remodeling during spermatogenesis. Although antibody- and MS-based approaches have been applied for characterization of PTMs on H3 variants during spermatogenesis, variant-specific PTMs are still underexplored. We identified several lysine modifications in H3 variants, including testis-specific histone H3 (H3t), through their successful separation with MS-based strategy, based on differences in masses, retention times, and presence of immonium ions. Besides methylation and acetylation, we detected formylation as a novel PTM on H3 variants in mouse testes. These patterns were also observed in H3t. Our data provide high-throughput structural information about PTMs on H3 variants in mouse testes and show possible applications of this strategy in future proteomic studies on histone PTMs.

1. Introduction

The nucleosome—the basic repeating element of the chromatin—consists of eight core histones and one linker histone wrapped by a DNA fragment. Histone variants encoded by different genes are diversely expressed during cell cycles [1–3]. Histone H3, one of the core histones, has a number of variants (H3.1, H3.2, H3.3, CENP-A, H3t, H3.X, H3. Y, and H3.5) that are characterized using proteomic approaches [4,5]. These histone H3 variants are subjected to post-translational modifications (PTMs) for regulation of several biological activities such as transcription and chromatin remodeling [4]. Proteomic approaches using antibody or mass spectrometry (MS) have facilitated detection of several PTMs such as methylation, acetylation, phosphorylation, O-GlcNAcylation, and ubiquitination on H3 variants [4]. The characterization of histone PTMs has traditionally relied on the antibody-based analysis, owing to its sensitivity; however, this method is associated with several shortcomings such as cross-reactivity and uncertain specificity. In particular, antibody-based approaches are unable to distinguish variants with similar but small alterations in their amino acid sequences [1–3,6].

Mass spectrometry has become a general and powerful tool ensuring rapid, sensitive, accurate, and comprehensive characterization of various PTMs of amino acid residues on histone variants [1–4,6,7]. In particular, MS-based bottom-up strategy involving a digestion step was reported to be unsuitable for comprehensive analysis, owing to the loss of information about PTMs of short peptides (3–4 amino acids) generated during digestion. However, recent advances with tandem mass spectrometry (MS/MS) provide sensitive analysis as well as high-throughput and informative data for identification of specific or novel modified sites on histones [2,6,7].

The expression of histone H3 variants, including H3t, has been detected during spermatogenesis [5,8]. Studies have reported the importance of acetylation and methylation of the N-terminal lysine residues of histone H3 in the regulation of chromatin structure during spermatogenesis [5,8]. Acetylated and methylated lysine as well as phosphorylated serine have been identified in H3 variants during spermatogenesis, using antibody-based techniques [9–13]. In addition, MS-based approaches characterized lysine modifications on H3 variants during spermatogenesis [14,15]; however, these methods have limited potential for identification of variant-specific and novel PTMs. The histone H3t is mainly enriched in small amounts from somatic cells during spermatogenesis [5,8]. Our previous study showed successful separation and characterization of H3t and its K9 mono-, di-, and tri-methylations from mouse testes, using top-down strategies [16].

Abbreviations: MS, mass spectrometry; PTMs, post-translational modifications; HCD, high-energy collision dissociation; TCA, trichloroacetic acid; DTT, dithiothreitol; H2SO4, sulfuric acid; HPLC, high performance liquid chromatography; RP, reverse phase; HFBA, heptafluorobutyric acid; SDS-PAGE, sodium dodecyl sulfate-polyacrylamide gel electrophoresis; TFA, trifluoroacetic acid; ESI-TRAP, electrospray TRAP; FDR, false discovery rate; MALDI, matrix-assisted laser desorption/ionization; ISD, in source decay

* Corresponding author.
E-mail address: dohmae@riken.jp (N. Dohmae).

http://dx.doi.org/10.1016/j.bbrep.2017.05.003
Received 20 April 2017; Accepted 23 May 2017
Available online 24 May 2017

However, no information on the comprehensive mapping of other PTMs on H3t has been reported. Studies on the identification of PTMs on histone H3 variants have become important for understanding the chromatin structure and its role in biological activities. Specific and comprehensive analysis is required to study the structure and PTMs of histone H3 variants during spermatogenesis.

In this study, we comprehensively characterized PTMs on H3 variants in mouse testes, using MS-based bottom-up approach. Our data showed global mapping of modified lysine in H3 variants. These patterns were observed not only at histone tails (K9, K14, K18, K23, K36, and K112) but also at K56 and K79. Most lysine sites were mainly methylated and acetylated. In addition, we identified formylation as a novel PTM on H3 variants in mouse testes by higher-energy collisional dissociation (HCD) fragmentation. We also observed these PTMs on H3t. Our approach enables high-throughput analysis of PTMs as well as differentiation of similar modified masses at the same lysine, such as tri-methylation versus acetylation on K9 and K27 and di-methylation versus formylation on K23. These data will be useful for the investigation of overall assessment of PTM on histones with accuracy and specificity.

2. Materials and methods

2.1. Extraction of histone H3 variants

Mouse (BALB/c) testes combined with epididymides, purchased from Funakoshi Co. (Tokyo, Japan), were homogenized following separation. Whole histones were extracted from testes and epididymides by the trichloroacetic acid (TCA) precipitation method with minor modifications [17]. Briefly, all steps were carried out at 4 °C. Testes (148.7 mg) and epididymides (183.9 mg) tissues were suspended in hypertonic lysis buffer (10 mM Tris-Cl pH 8.0, 1 mM KCl, 1.5 mM Mg $(CH_3COO)_2$, 1 mM dithiothreitol [DTT], and protease inhibitors) for 30 min. Lysed cells were centrifuged at 10,000 $\times g$ for 10 min and the pelleted intact nuclei resuspended in 0.4 N sulfuric acid (H_2SO_4) for 30 min. The nuclear debris was pelleted by centrifugation at 16,000 $\times g$ for 10 min to obtain a supernatant enriched with histones. The supernatant was precipitated by incubation with TCA at a final concentration of 33% for 30 min. The precipitate was subjected to centrifugation at 16,000 $\times g$ for 10 min. The histone pellet thus obtained was washed with acetone, dried at room temperature, and resuspended in 100 µL MilliQ water.

2.2. Separation of each H3 variant by high performance liquid chromatography (HPLC)

Histone H3 variants were separated with Agilent HPLC 1100 series (Agilent Technologies, Santa Clara, CA, USA), using a C4 reverse-phase (RP) column (2.0 mm × 15.0 mm, 3-µm particle size; GL sciences, Tokyo, Japan). A 20-µL sample was injected and detected at UV wavelength of 215 nm. Heptafluorobutyric acid (HFBA, Thermo-Fisher Scientific, Waltham, MA, USA) was used as an ion-pairing reagent. The mobile phase A (5% acetonitrile with 0.1% HFBA) and B (90% acetonitrile with 0.1% HFBA) were delivered at a flow rate of 0.1 mL/min, using the following gradient parameters: 0 min (to 5 min, 15% solvent B); 5 min (to 15 min, 15–48% solvent B); 15 min (to 25 min, 48% solvent B); 25 min (to 100 min, 48–62% solvent B); 100 min (to 120 min, 62–100% solvent B); 120 min (to 130 min, 100% solvent B); 130 min (to 135 min, 100–15% solvent B); 135 min (to 145 min, 15% solvent B). The fraction collector (Gilson, Middleton, WI, USA) was programmed to collect fractions from 30 to 116 min at an interval of 1 min.

2.3. In-gel digestion

Each band containing histone proteins was excised from the sodium dodecyl sulfate-polyacrylamide gel electrophoresis (SDS-PAGE) gel and destained using 30% acetonitrile. Disulfide bonds of proteins were reduced with 50 mM DTT at 37 °C for 2 h, followed by their alkylation with 100 mM acrylamide at room temperature for 30 min. Histones were subjected to digestion by incubation of gel pieces with 20 µL of buffer (20 mM Tris-HCl, pH 8.0) and trypsin (0.01 µg/µL) at 37 °C for 12–15 h.

2.4. Characterization of PTMs by MS

After digestion, the sample was analyzed by a Q-Exactive mass spectrometer (Thermo-Fisher Scientific, Bremen, Germany) with HCD using a linear gradient of 0–100% solvent B over 30 min (solvent A: 0.1% trifluoroacetic acid [TFA]; solvent B: 80% acetonitrile with 0.1% TFA). The MS was directed using Xcalibur software version 3.0.63 (Thermo-Fisher Scientific). A nanoelectrospray (Thermo-Fisher Scientific) was applied with a spray voltage of 1.9 kV and capillary temperature of 275 °C. We acquired HCD spectra (at a range of 300–2000 m/z) with a resolution of 70,000 at m/z 400 Da. MS/MS spectra were obtained in a data-dependent manner. Spectra of histone peptides were searched against the protein databases (NCBInr and SWISS-PROT), using the MASCOT program (version 2.5, Matrix Science, UK).

2.5. Data processing

We processed MS/MS files as *.mgf files, using Proteome Discoverer (version 2.1.0.81, Thermo-Fisher Scientific). Converted files were searched through MASCOT against the databases (NCBI and SWISS-PROT), using following parameters: monoisotopic mass values; trypsin as the enzyme for digestion, with two missed cleavages; 1.2 Da of peptide mass tolerance; and 0.02 Da of fragment mass tolerance. Peptide charge was set at +1, +2, and +3 and the instrument set to electrospray iontrap (ESI-TRAP) with decoy mode. Variable modifications were as follows: mono- (+14.016 Da), di- (+28.031 Da), tri-methylation (+42.047 Da), formylation (+27.995 Da), acetylation (+42.011 Da), propionylation (+56.026 Da), and butyrylation (+70.042 Da) of lysine and oxidation (+15.995 Da) of methionine. Identified peptides were approved at a false discovery rate (FDR) less than 1%, with a minimum score of 15. HCD spectra were manually examined for exact characterization of poor matched results from MASCOT search data.

3. Results and discussion

3.1. Separation of histone H3 variants

We successfully separated histone H3 variants from mouse testes and epididymides, using HPLC with HFBA (Fig. 1). In our past study, we had employed MS-based analysis for verification of each separated histone H3 variant [16,18]. Epididymis is a tube connected to the testis where sperms flow and get temporarily stored [5]. We used epididymides to compare patterns of H3 histone variants, including H3t, during spermatogenesis. H3t was clearly separated in mouse testes and undetectable in the epididymides (Fig. 1). In addition, higher H3.2 signal was observed in the epididymides compared to that in the testes (Fig. 1).

3.2. Identification of PTMs on H3 variants in mouse testes

We characterized PTMs on H3.1, H3.2, H3.3, and H3t, using MS-based bottom-up approach. Several studies have employed antibody-based immunoassays for the identification of PTMs such as methylation and acetylation during spermatogenesis, owing to their sensitivity. However, antibody-based assays exhibit cross-reactivity and uncertain specificity, which limit their application for high-throughput PTM

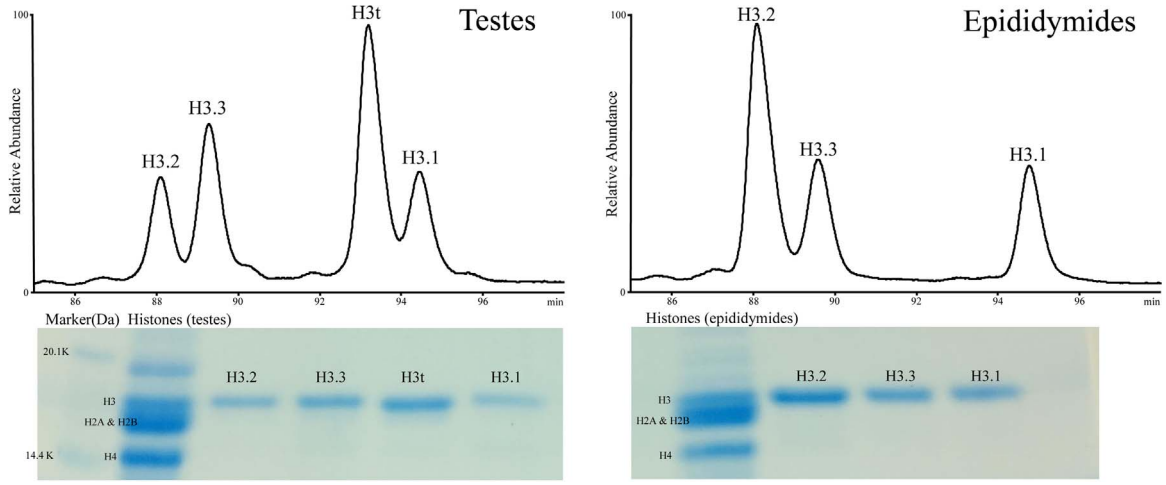

Fig. 1. Separation of histone H3 variants from mouse testes and epididymides. Histone H3 variants were separated by liquid chromatography using a C4 revered-phase column and an ion-pairing reagent. In-gel digestion using trypsin was performed to isolate and analyze each separated histone before instrumental analysis. Histone H3 variants were identified using the method established in our previous study.[16,18].

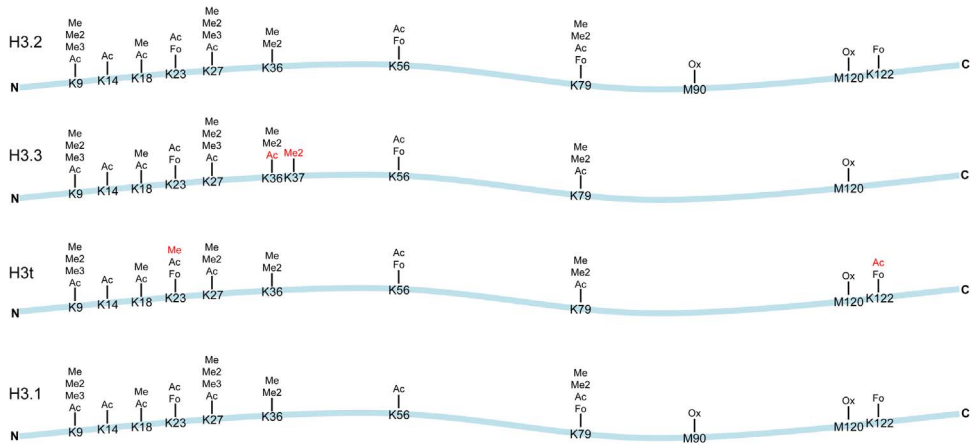

Fig. 2. Post-translational modifications (PTMs) on H3 variants from mouse testes. PTMs on each H3 variant were identified using higher-energy collisional dissociation fragmentation. Mass spectra were matched using MASCOT search engine (version 2.5, Matrix Science, UK) from the databases (NCBI for H3t and SWISS-PROT for other H3 variants). Me: methylation; Ac: acetylation; Fo: formylation; Ox: oxidation.

analysis [1,2,6,9–13]. Mass spectrometry-based analysis has become a universal and powerful tool for characterization of PTMs on histones [1,2,6,7], and several MS-based approaches have been developed for identification of specific modifications on histone variants during spermatogenesis [14–16,18–23]. In addition, PTMs on H3 variants have been performed to verify their structural features [14–16]. However, these methods provide unclear results and have limited potential to identify variant-specific (e.g., H3t) and novel PTMs [14–16]. Our MS-based bottom-up approach enabled high-throughput identification of PTMs on H3 variants (H3.1, H3.2, H3.3, and H3t), which were specifically separated with ion-pair reagent by HPLC.

We employed HCD fragmentation for identification of PTMs on H3 variants in mouse testes (Fig. 2). Each modification was characterized through MASCOT search engine against databases (NCBI and SWISS-PROT). Several PTMs, including methylation, acetylation, formylation, and butyrylation, of lysines in H3 variants were observed (Fig. 2). During spermatogenesis, several PTMs such as acetylation, methylation, phosphorylation, ubiquitylation, SUMOylation, and PARylation have been detected on H3 variants. Proteomic approaches revealed methylations of lysine and arginine, acetylation of lysine, and phosphorylation of serine [5,8]. Methylations of K9 and K27 at the N-terminus are known as repressive factors in chromatin structures [5,8,24]. Antibody- and MS-based approaches have been employed for identification of these modifications at the N-terminus of H3 histone of the testes during spermatogenesis [9,11,12,14,16]. Our results revealed methylation of not only the N-terminal K9 and K27 residues but also the K79 residue (Fig. 2). In addition, we also detected various acetylated sites such as K9, K14, K18, K24, K27, K36 (H3.3), K56, K79, and K122 (H3t) (Fig. 2). A recent study reported comprehensive characterization of methylations and acetylation on H3 variants, including H3.1 and H3.3, during spermatogenesis [15]. However, this study failed to detect PTMs such as mono-methylation of K4, R26, and R53, di-methylation of K18 and K23, as well as tri-methylation of K36 and K37 in the sequences of H3 variants observed in our study (Fig. 2) [15]. We identified each PTM from four separated H3 variants (H3.1, H3.2, H3.3, and H3t) in mouse testes (Fig. 2). Most PTMs were detected at the same site for each H3 histone variant. In addition, we also detected variant-specific PTMs such as K23 methylation and K122 acetylation in H3t as well as K36 acetylation and K37 di-methylation in H3.3 (Fig. 2). Furthermore, we identified formylation as a novel PTM (Fig. 2). Formylation of lysine residues that also undergo acetylation and methylation (for chromatin remodeling and transcription regulation) has been identified on histone H3 in mammalian cells by MS [4,25]. However, formylation of lysine during spermatogenesis has not been reported. We characterized formylation of lysine in H3 variants in mouse testes by MS-based analysis (Fig. 2).

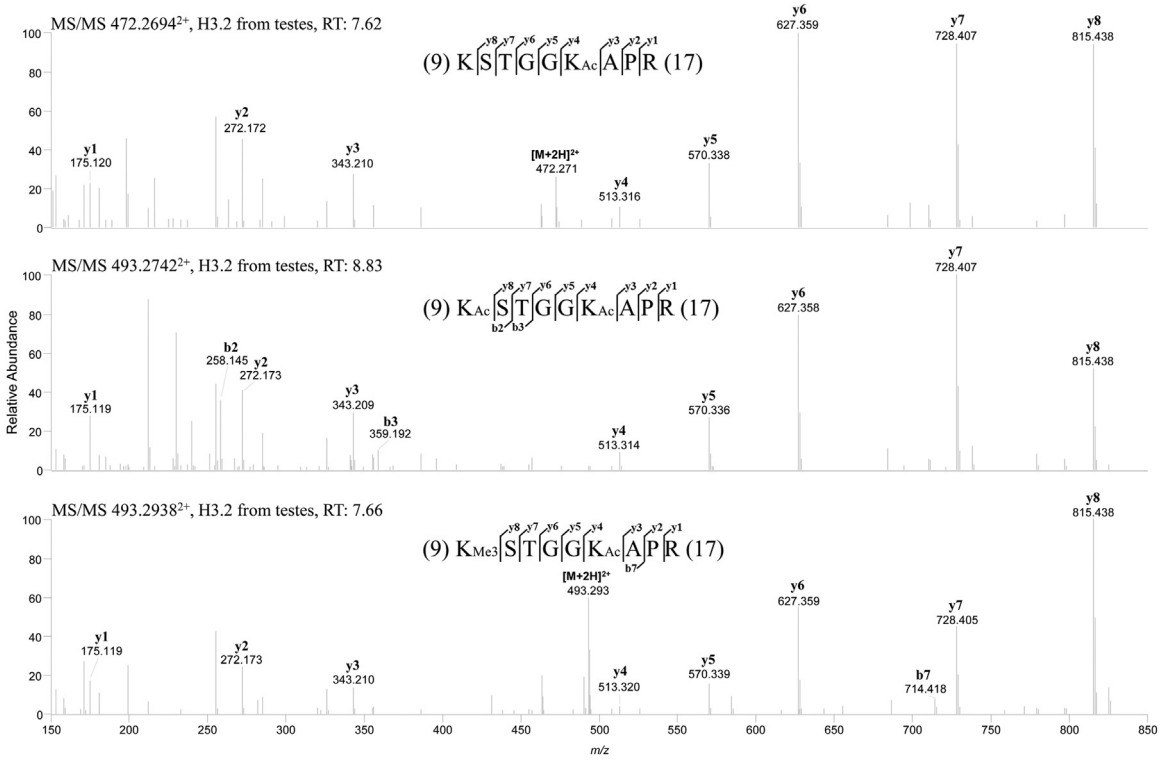

Fig. 3. Identification of acetylation (Ac, 42.0106 Da) versus tri-methylation (Me3, 42.0495 Da). Peptides ($_{9}$KSTGGKAPR$_{17}$) with post-translational modifications (Ac and Me3) were characterized using higher-energy collisional dissociation (HCD) fragmentation. Mass spectra were matched using MASCOT search engine from the databases (NCBI for H3t and SWISS-PROT for other H3 variants). HCD spectra were manually examined for exact characterization of poorly matched results from MASCOT search data.

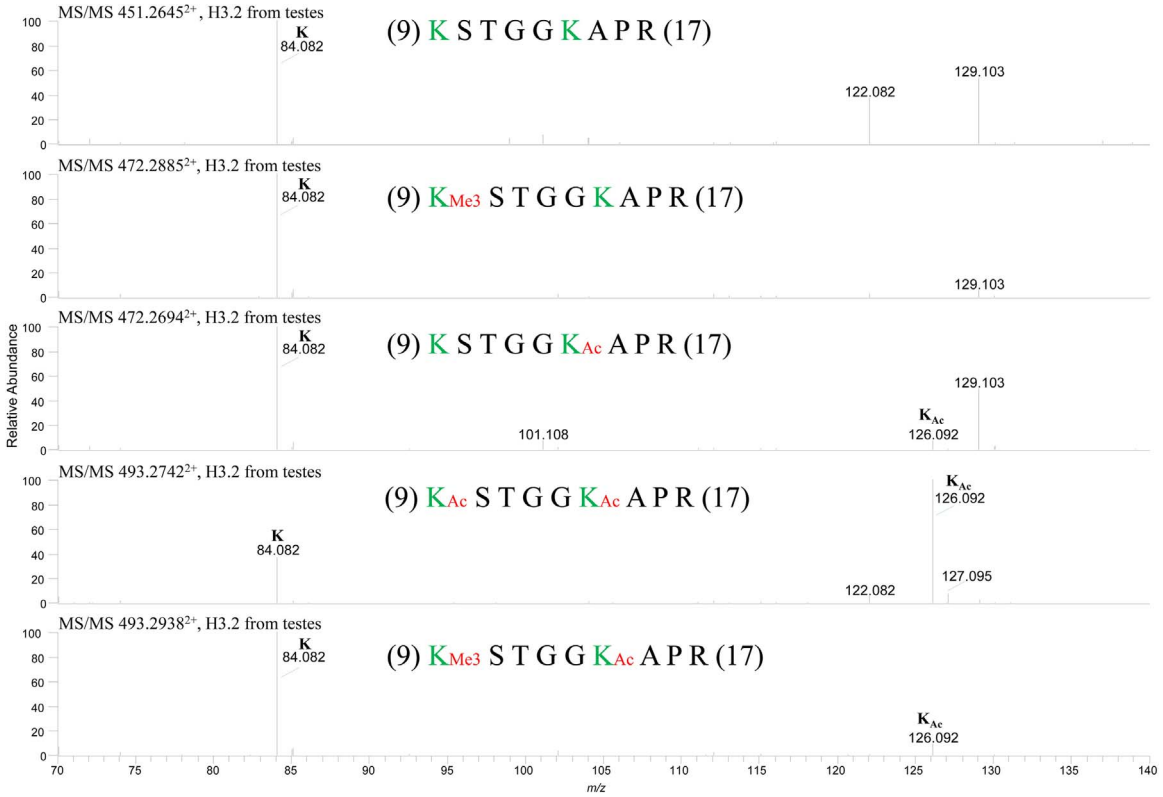

Fig. 4. Comparison of immonium ions from acetylated and tri-methylated lysines of H3 peptides. Peptides ($_{9}$KSTGGKAPR$_{17}$) with post-translational modifications (Ac: acetylation and Me3: tri-methylation) were characterized using higher-energy collisional dissociation fragmentation. Immonium ions of lysine acetylation at *m/z* 126.092 were detected from acetylated peptides ($_{9}$KSTGGK$_{Ac}$APR$_{17}$, $_{9}$K$_{Ac}$STGGK$_{Ac}$APR$_{17}$, and $_{9}$K$_{Me3}$STGGK$_{Ac}$APR$_{17}$) in H3 variants. A diagnostic immonium ion of lysine at *m/z* 84.082 was detected.

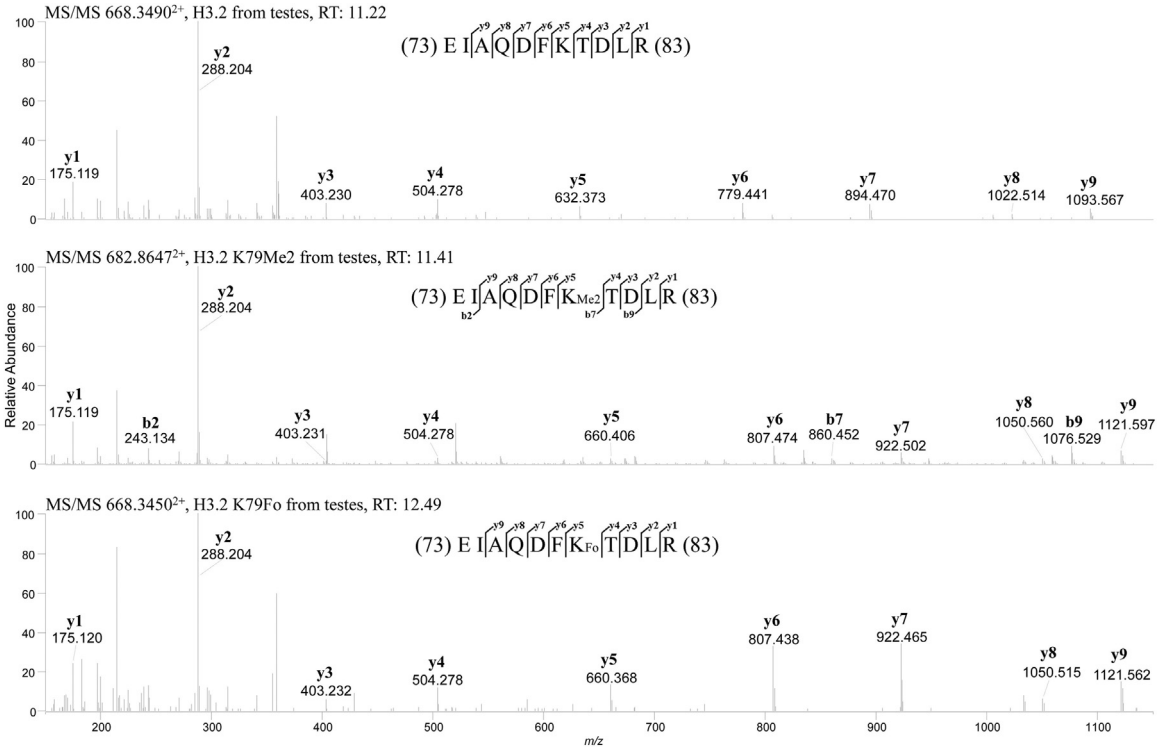

Fig. 5. Identification of formylation (Fo, 27.9949 Da) versus tri-methylation (Me2, 28.0313 Da). Peptides ($_{73}$EIAQDFKTDLR$_{83}$) with post-translational modifications (Fo or Me2) were characterized using higher-energy collisional dissociation (HCD) fragmentation. Mass spectra were matched using MASCOT search engine from the database (NCBI for H3t and SWISS-PROT for other H3 variants). HCD spectra were manually examined for exact characterization of poor matched results from MASCOT search data.

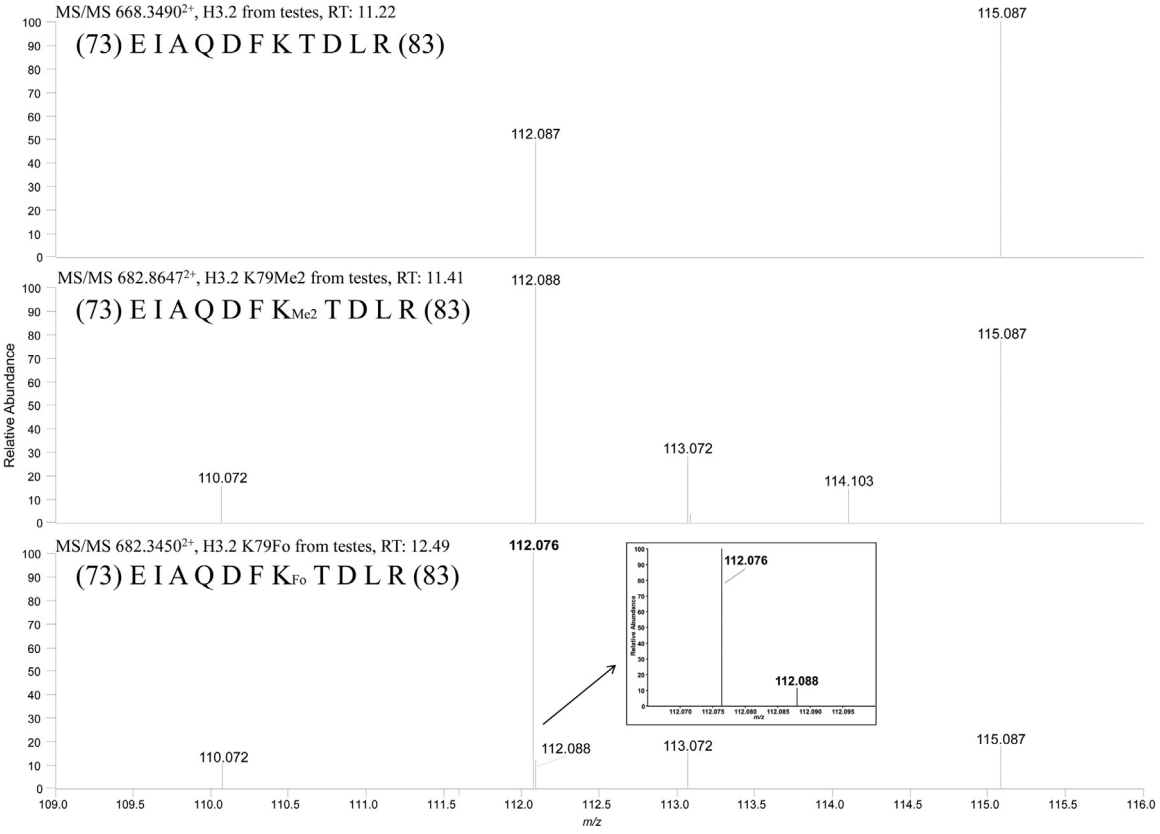

Fig. 6. Detection of immonium ions of formylated lysine. Peptides ($_{73}$EIAQDFKTDLR$_{83}$) with post-translational modifications (Fo: formylation or Me2: di-methylation) were characterized using higher-energy collisional dissociation fragmentation. Immonium ions of formylated lysine at *m/z* 112.076 were observed from the peptides ($_{73}$EIAQDFK$_{Fo}$TDLR$_{83}$) of H3 variants.

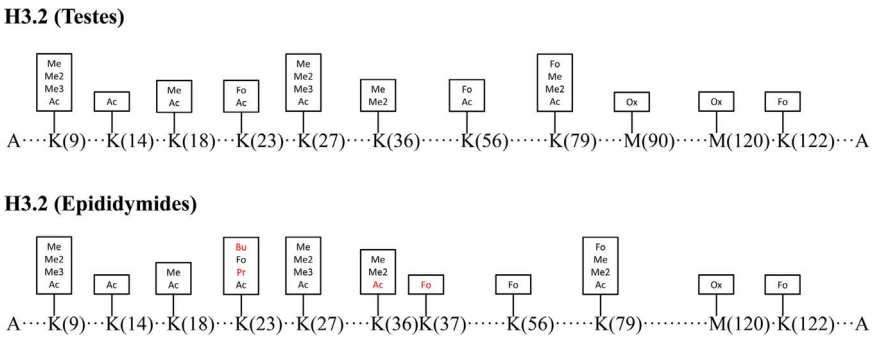

Fig. 7. Comparison of post-translational modifications (PTMs) on H3.2 between mouse testes and epididymides. PTMs on each H3 variant were identified using higher-energy collisional dissociation fragmentation from the tryptic-digested peptides. Mass spectra were matched using MASCOT search engine from the databases (NCBI for H3t and SWISS-PROT for other H3 variants). Me: methylation; Ac: acetylation; Fo: formylation; Bu: butyrylation; Ox: oxidation.

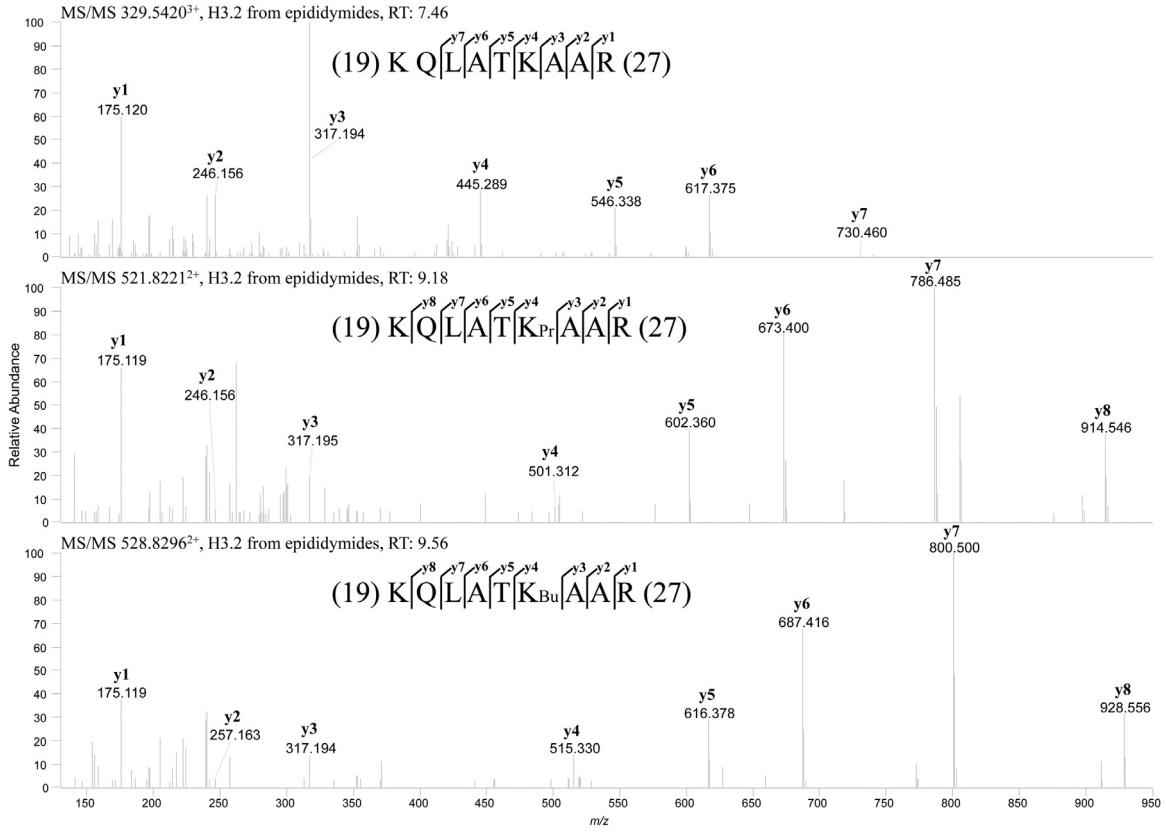

Fig. 8. MS/MS spectra of propionylated and butyrylated K23 in H3.2 from the mouse epididymides. Peptides ($_{19}$KQLATKAAR$_{27}$) with post-translational modifications (Pr: propionylation or Bu: butyrylation) were characterized using higher-energy collisional dissociation fragmentation. Mass spectra were matched using MASCOT search engine from the database (SWISS-PROT).

3.3. Comprehensive characterization of PTMs on H3t

The characterization of PTMs is an important process to study the structural features of modified sites on proteins for understanding their association with epigenetic regulation. Testis-specific histone H3t is mainly expressed and enriched during spermatogenesis, with a low-level expression detected in normal tissues [5,8]. Our previous work offers insight into the identification of such K9 mono-, di-, and tri-methylations on H3t with the top-down strategy using matrix-assisted laser desorption/ionization (MALDI)-in source decay (ISD) [16]. The characterization of other modified sites on H3t during spermatogenesis has been underexplored. In this study, we explored PTMs on H3t with bottom-up approach using HCD fragmentation (Fig. 2). The sequence of testis-specific histone H3t was aligned in a previous report [26]. In our previous study, we had successfully separated H3t from mouse testes and characterized its K9 methylations using the MS-based top-down approach [16,18]. In this study, several modified lysines were identified in H3t from mouse testes. We detected mono- (K9, K18, K23, K27, K36, and K79), di- (K9, K27, K36, and K79), and tri-methylation (K9), as well as acetylation (K9, K14, K18, K23, K27, K56, K79, and K122), formylation (K23, K56, and K122), and oxidation (K122) in H3t, and observed similar patterns in other H3 variants (with an exception of K23 methylation and K122 acetylation). Thus, acetylation was also observed at the same lysine residues (Fig. 2). In comparison to other variants, H3t showed no tri-methylation of K27. In addition, we identified formylation of K23, K56, and K112 as novel modified sites on H3t in this study (Fig. 2). These results from the foundation for the structural research of PTMs on H3t.

3.4. Determination of PTMs with similar molecular masses

We identified PTMs with similar molecular masses at same lysine

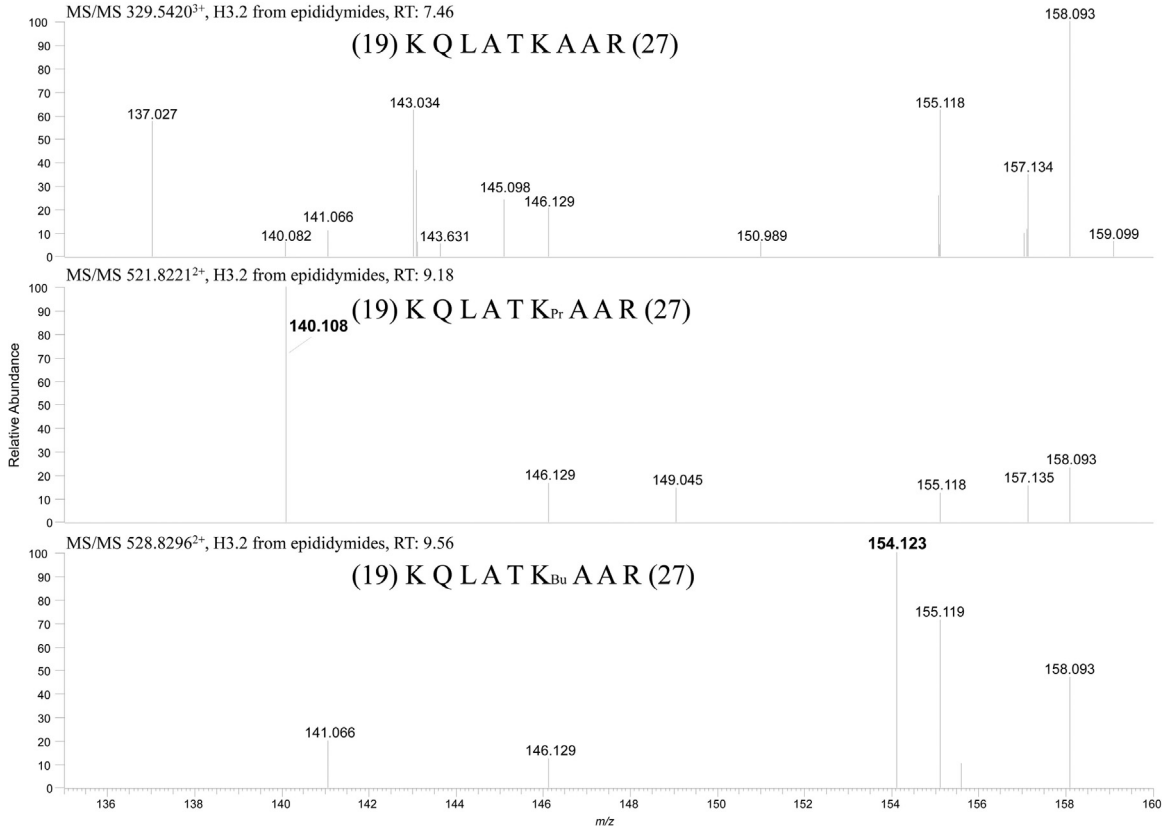

Fig. 9. Immonium ions of propionylated and butyrylated K23 in H3.2 from the epididymides. Peptides ($_{19}$KQLATKAAR$_{27}$) with post-translational modifications (Pr: propionylation or Bu: butyrylation) were characterized using HCD fragmentation. Immonium ions of propionylated and butyrylated lysine at *m/z* 140.108 and 154.123, respectively, were observed from the peptides ($_{19}$KQLATK$_{Pr}$AAR$_{27}$ and $_{19}$KQLATK$_{Bu}$AAR$_{27}$) of H3 variants.

residues (K9, K27, and K79) in H3 variants (Fig. 2). Acetylation (42.0106 Da) versus tri-methylation (42.0470 Da) and formylation (27.9949 Da) versus di-methylation (28.0313 Da) are attributed with similar change in the molecular mass of the lysine residue [2]. The characterization of these PTMs on histone variants has been challenging [2,6,27,28]. We identified acetylation versus tri-methylation and formylation versus di-methylation from MS/MS spectra generated using HCD fragmentation (Figs. 3, 4). For instance, acetylation and tri-methylation of K9 versus both acetylations of K14 on H3.2 peptides ($_9K_{Me3}STGGK_{Ac}APR_{17}$ = 493.2938^{2+} and $_9K_{Ac}STGGK_{Ac}APR_{17}$ = 493.2742^{2+}, respectively) of H3.2 were identified at retention times of 8.83 and 7.66 min, respectively (Fig. 3). The mass difference was 42.0488 Da between K9 and K14 acetylation ($_9K_{Ac}STGGK_{Ac}APR_{17}$) and K14 acetylation ($_9KSTGGK_{Ac}APR_{17}$ = 472.2694^{2+}) and 42.0096 Da between K9 tri-methylation ($_9K_{Me3}STGGK_{Ac}APR_{17}$) and K14 acetylation ($_9KSTGGK_{Ac}APR_{17}$). In addition, the immonium ion at *m/z* 126 was mainly detected as the specific diagnostic ion of lysine acetylation fragmented by collision-induced dissociation in contract with tri-methylation [29–31]. Peptides acetylated at K9 and (or) K14 showed the immonium ion at *m/z* 126.092 compared to the unmodified H3 variants or those with tri-methylated lysine (Fig. 4). In this study, formylation and demethylation of the same lysine (K79) in H3.1 and H3.2 were successfully identified from y-ions fragmented using HCD at different retention times (Fig. 5). Formylation specifically forms immonium ion at *m/z* 112 compared with di-methylation, as reported in a previous study [32,33]. Formylation of immonium ion at *m/z* 112.076 was also observed in our results (Fig. 6). Using HCD fragmentation, we classified acetylation versus tri-methylation and formylation versus di-methylation at same lysine residues of H3 variants on the basis of different masses, retention times, and existence of immonium ions. These results will be helpful in differentiation of PTMs with similar molecular masses at same lysine residues of histone H3 variants.

3.5. Characterization of propionylation and butyrylation on histone H3 variant

Propionylation (56.0262 Da) and butyrylation (70.0418 Da) were undetectable in H3 variants from mouse testes; however, HCD fragmentation revealed these PTMs of K23 on H3 variants from mouse epididymides (Fig. 7). Previous studies have detected histone H3 with immonium ion of propionyl lysine (K23) at *m/z* 140.106 in yeast and mammalian cells using collision-induced dissociation fragmentation [34,35]. The MS/MS spectrum of the peptide 19KQLATKPrAAR27 revealed the immonium ion of propionyl lysine at *m/z* 140.108 on K23 in H3 variants (Fig. 8). Previous MS-based analyses have identified butyrylated lysine in H3 variants [34,36,37]. We observed butyrylation of K23 in H3 variants from mouse epididymides (Fig. 8). Using HCD fragmentation, we identified immonium ion of butyrylated K23 at *m/z* 154.123, which is undetected in unmodified or propionylated peptides (19KQLATKAAR27) (Fig. 9). This motif showed approximately 14.015 Da mass difference (theoretically 14.016 Da) from that of the immonium ion of lysine propionylation. The characterization of immonium ion of histone butyrylation has been incompletely explored. Our results will be useful for differentiation of PTMs, including butyrylation, on lysine.

4. Conclusions

Our data demonstrate comprehensive characterization of PTMs on successfully separated H3 variants, including H3t, using MS-based bottom-up approach. Several lysine PTMs such as mono-, di-, and tri-methylation as well as acetylation and formylation were identified on the basis of different masses, retention times, and existence of

immonium ions generated by HCD fragmentation. These specific and novel motifs were also detected on H3t, specifically expressed during spermatogenesis. Our approach not only enabled differentiation of similar PTM masses (acetylation versus tri-methylation) but also allowed characterization of other modified patterns, including butyrylation and propionylation, on H3 variants from mouse epididymides. Our MS-based strategy can be applied to other samples and it will be helpful for detailed comprehensive analysis of PTM on histone variants as well as in the discovery of other novel or specific PTMs during spermatogenesis in future proteomic research.

This research did not receive any specific grant from funding agencies in the public, commercial, or not-for-profit sectors.

Appendix A. Transparency document

Supplementary data associated with this article can be found in the online version at http://dx.doi.org/10.1016/j.bbrep.2017.05.003.

References

[1] B.A. Garcia, J. Shabanowitz, D.F. Hunt, Characterization of histones and their post-translational modifications by mass spectrometry, Curr. Opin. Chem. Biol. 11 (2007) 66–73.
[2] A. Moradian, A. Kalli, M.J. Sweredoski, S. Hess, The top-down, middle-down, and bottom-up mass spectrometry approaches for characterization of histone variants and their post-translational modifications, Proteomics 14 (2014) 489–497.
[3] Y. Zheng, X. Huang, N.L. Kelleher, Epiproteomics: quantitative analysis of histone marks and codes by mass spectrometry, Curr. Opin. Chem. Biol. 33 (2016) 142–150.
[4] Y.M. Xu, J.Y. Du, A.T.Y. Lau, Posttranslational modifications of human histone H3: an update, Proteomics 14 (2014) 2047–2060.
[5] C. Rathke, W.M. Baarends, S. Awe, R. Renkawitz-Pohl, Chromatin dynamics during spermiogenesis, Biochim. Biophys. Acta 2014 (1839) 155–168.
[6] X. Su, C. Ren, M.A. Freitas, Mass spectrometry-based strategies for characterization of histones and their post-translational modifications, Expert Rev. Proteom. 4 (2007) 211–225.
[7] A.,M. Arnaudo, B.A. Garcia, Proteomic characterization of novel histone post-translational modifications, Epigenetics Chromatin 6 (2013) 24.
[8] M.T. Bedford, J. Bao, Epigenetic regulation of the histone-to-protamine transition during spermiogenesis, Reproduction 151 (2016) R55–R70.
[9] C. Rathke, S. Jayaramaiah-Raja, M. Bartkuhn, R. Renkawitz, R. Renkawitz-Pohl, Transition from a nucleosome-based to a protamine-based chromatin configuration during spermatogenesis in Drosophila, J. Cell Sci. 120 (2007) 1689–1700.
[10] M. Godmann, V. Auger, V. Ferraroni-Aguiar, A. Di Sauro, C. Sette, R. Behr, S. Kimmins, Dynamic regulation of histone H3 methylation at lysine 4 in mammalian spermatogenesis, Biol. Reprod. 77 (2007) 754–764.
[11] N. Song, J. Liu, S. An, T. Nishino, Y. Hishikawa, T. Koji, Immunohistochemical analysis of histone H3 modifications in germ cells during mouse spermatogenesis, Acta Histochem. Cytochem. 44 (2011) 183–190.
[12] M. De Vries, L. Ramos, Z. Housein, P. De Boer, Chromatin remodeling initiation during human spermatogenesis, Biol. Open 1 (2012) 446–457.
[13] K. Kamodiya, A.R. Krebs, M. Oulad-Abdelghani, H. Kimura, L. Tora, H3K9 and H3K14 acetylation co-occur at many gene regulatory elements, while H3K14ac marks a subset of inactive inducible promoters in mouse embryonic stem cells, BMC Genom. 13 (2012) 424.
[14] B.A. Garcia, C.E. Thomas, N.L. Kelleher, C.A. Mizzen, Tissue-specific expression and post-translational modification of histone H3 variants, J. Proteome Res. 7 (2008) 4225–4236.
[15] L.J. Luense, X. Wang, S.B. Schon, A.H. Weller, E.L. Shiao, J.M. Bryant, M.S. Bartolomei, C. Coutifaris, B.A. Garcia, S.L. Berger, Comprehensive analysis of histone post-translational modifications in mouse and human male germ cells, Epigenetics Chromatin 9 (2016) 24.
[16] H.–G. Kwak, N. Dohmae, Characterization of post-translational modifications on lysine 9 of histone H3 variants in mouse testis using matrix-assisted laser desorption/ionization-in source decay, Rapid Commun. Mass Spectrom. (2016), http://dx.doi.org/10.1002/rcm.7742 (Epub ahead of print).
[17] D. Shechter, H.L. Dormann, D.C. Allis, S.B. Hake, Extraction, purification and analysis of histones, Nat. Protoc. 2 (2007) 1445–1457.
[18] H.–G. Kwak, N. Dohmae, Proteomic characterization of histone variants in the mouse testis by mass spectrometry-based top-down analysis, Biosci. Trends 10 (2016) 357–364.
[19] K.L. Rose, A. Li, I. Zalenskaya, Y. Zhang, E. Unni, K.C. Hodgson, Y. Yu, J. Shabanowitz, M.L. Meistrich, D.F. Hunt, J. Ausio, C-terminal phosphorylation of murine testis-specific histone H1t in elongating spermatids, J. Proteome Res. 7 (2008) 4070–4078.
[20] B. Sang, S. Chwatal, H. Talasz, H.H. Lindner, Testis-specific linker histone H1t is multiply phosphorylated during spermatogenesis, J. Biol. Chem. 284 (2009) (3610-3608).
[21] S. Lu, Y.M. Xie, X. Li, J. Luo, X.Q. Shi, X. Hong, Y.H. Pan, X. Ma, Mass spectrometry analysis of dynamic post-translational modifications of TH2B during spermatogenesis, Mol. Hum. Reprod. 5 (2009) 373–378.
[22] S.K. Pentakota, S. Sandhya, A.P. Sikarwar, N. Chandra, M.R. Satyanarayana Rao, Mapping post-translational modifications of mammalian testicular specific histone variant TH2B in tetraploid and haploid germ cells and their implications on the dynamics of nucleosome structure, J. Proteome Res. 13 (2014) 5603–5617.
[23] M. Samson, M.M. Jow, C.C. Wong, C. Fitzpatrick, A. Aslanian, I. Saucedo, R. Estrada, T. Ito, S.K. Park, J.R. Yates 3rd, D.S. Chu, The specification and global reprogramming of histone epigenetic marks during gamete formation and early embryo development in *C. elegans*, PLoS One 10 (2014) e1004588.
[24] L. Ly, D. Chan, J.M. Trasler, Developmental windows of susceptibility for epigenetic inheritance through the male germline, Semin. Cell Div. Biol. 43 (2015) 96–105.
[25] J.R. Wisniewski, A. Zougman, M. Mann, Nepsilon-formylation of lysine is a widespread post-translational modification of nuclear proteins occurring at residues involved in regulation of chromatin function, Nucleic Acids Res. 36 (2008) 570–577.
[26] K. Maehara, A. Harada, Y. Sato, K.I. Mathumoto, H. Kimura, Y. Ohkawa, Tissue-specific expression of histone H3 variants diversified after species separation, Epigenetics Chromatin 8 (2015) 35.
[27] J.A. Oses-Prieto, X. Zhang, A.L. Burlingame, Formylation of epsilon-formyllysine on silver-stained proteins: implications for assignment of isobaric demethylation sites by tandem mass spectrometry, Mol. Cell Proteom. 6 (2007) 181–192.
[28] K. Contrepois, E. Ezan, C. Mann, F. Fenaille, Ultra-high performance liquid chromatography-mass spectrometry for the fast profiling of histone post-translational modifications, J. Proteome Res. 9 (2010) 5501–5509.
[29] J.–Y. Kim, K.–W. Kim, H.–J. Kwon, D.–W. Lee, J.–S. Yoo, Probing lysine acetylation with a modification-specific marker ion using high-performance liquid chromatography/electrospray-mass spectrometry with collision-induced dissociation, Anal. Chem. 74 (2002) 5443–5449.
[30] K. Zhang, P.M. Yau, B. Chandrasekhar, R. New, R. Kondrat, B.S. Imai, M.E. Bradbury, Differentiation between peptides containing acetylated or tri-methylated lysines by mass spectrometry: an application for determining lysine 9 acetylation and methylation of histone H3, Proteomics 4 (2004) 1–10.
[31] M.B. Trelle, O.N. Jensen, Utility of immonium ions for assignment of epsilon-N-acetyllysine-containing peptides by tandem mass spectrometry, Anal. Chem. 80 (2008) 3422–3430.
[32] K.A. Dave, B.R. Hamilton, T.P. Wallis, S.G.B. Furness, M.L. Whitelaw, J.J. Gorman, Identification of *N,N*ε-dimethyl-lysine in the murine dioxin receptor using MALDI-TOF/TOF- and ESI-LTQ-Orbitrap-FT-MS, Int. J. Mass Spec. 268 (2007) 168–180.
[33] C.D. Kelstrup, C. Frese, A.J. Heck, J.V. Olsen, M.L. Nielsen, Analytical utility of mass spectral binning in proteomic experiments by SPectral Immonium Ion Detection (SPIID), Mol. Cell. Proteom. 13 (2014) 1914–1924.
[34] K. Zhang, Y. Chen, Z. Zhang, Y. Zhao, Identification and verification of lysine propionylation and butyrylation in yeast core histones using PTMap software, J. Proteome Res. 8 (2009) 900–906.
[35] B. Lui, Y. Lin, A. Darwanto, X. Song, G. Xu, K. Zhang, Identification and characterization of propionylation at histone H3 lysine 23 in mammalian cells, J. Biol. Chem. 284 (2009) 32288–32295.
[36] R.Y. Tweedie-Cullen, A.M. Brunner, J. Grossmann, S. Mohanna, D. Sichau, P. Nanni, C. Panse, I.M. Mansuy, Identification of combinational patterns of post-translational modifications on individual histones in the mouse brain, PLoS One 7 (2012) e36980.
[37] G. Xu, J. Wang, Z. Wu, L. Qian, L. Dai, X. Wan, M. Tan, Y. Zhao, Y. Wu, SAHA regulates histone acetylation, butyrylation, and protein expression in neuroblastoma, J. Proteome Res. 13 (2014) 4211–4219.